

Ferromagnetic-paramagnetic phase transition in manganite perovskites: Thermal hysteresis

S. W. Biernacki*

Institute of Physics, Polish Academy of Sciences, Aleja Lotnikow 32/46, 02-668 Warsaw, Poland

(Received 15 May 2003; revised manuscript received 30 June 2003; published 12 November 2003)

Using a phenomenological model we study the first- and second-order phase transitions in the $A_{1-x}M_x\text{MnO}_3$ system, with $x \approx 1/3$. The free energy in the vicinity of transition point is investigated. The continuous and discontinuous behavior of the order parameter is calculated, depending on the initial values of two model parameters. The thermal hysteresis is calculated for the order parameter and the entropy. The order of transition related to the magnetization and specific-heat measurements is discussed. The obtained theoretical and numerical results are used to consider the controversies on the nature of the phase transition in lanthanum manganites.

DOI: 10.1103/PhysRevB.68.174417

PACS number(s): 64.60.Cn, 75.40.Cx, 75.10.Hk, 75.50.Dd

I. INTRODUCTION

The manganese-based perovskites, such as $A_{1-x}M_x\text{MnO}_3$ (A is a trivalent rare-earth ion, M is divalent alkali-earth ion), have recently been the subject of intensive investigation.¹⁻³ They exhibit unusual and potentially useful magnetic properties, for example, the colossal magnetoresistance effect. The system with a nominal doping of $0.2 \leq x \leq 0.5$ undergoes a ferromagnetic to paramagnetic (FP) phase transition at the Curie temperature T_C . Recently, the character of the magnetic transition in these materials has been examined in a number of papers. Despite the efforts made, the nature of magnetic transition in some cases is controversial. In most cases the magnetic transition is of the second order. The measurements of magnetization in the $\text{La}_{0.67}\text{Ca}_{0.33}\text{MnO}_3$ showed small thermal hysteresis (about 5 K).⁴ Ghivelder *et al.*⁵ suggest that sharp peak of the specific heat in this material may indicate the first-order phase transition. However, the data on the magnetization in Refs. 4 and 5 appear to be continuous when approaching the transition point. Gordon *et al.*⁶ analyzed similar data for the $\text{La}_{0.65}\text{Ca}_{0.35}\text{MnO}_3$ sample and they suggested that these data are consistent with the Clausius-Clapeyron equation. This fact points to the first-order character of transition. On the other hand, Zhao *et al.*⁷ analyzed their data on the expansion coefficient and on the specific heat of $\text{La}_{0.67}\text{Ca}_{0.33}\text{MnO}_3$ crystal together with data for dT_C/dP . They suggested that these data are consistent with the Ehrenfest equation. Hence, they concluded that the phase transition is of the second order. The measurements of muon spin relaxation in the $\text{La}_{0.67}\text{Ca}_{0.33}\text{MnO}_3$, which probe the microscopic development of the magnetic order parameter, point to the second-order transition.⁸ Recently, the measurements of magnetization^{6,9,10} were also used to distinguish between the first-order and the second-order behavior. These measurements allow to determine the slope of isotherm plots of H/M vs M^2 , M being the measured magnetization and H the magnetic field. A positive slope indicates a second-order transition. However, the H/M graphs do not necessarily resolve the controversy related to the nature of phase transition in these materials. Therefore, in this paper, the model analysis of the first-order phase transition for the $A_{1-x}M_x\text{MnO}_3$ system is performed. The hysteretic character of the first-order magnetic phase transition is described using

the phenomenological model of the spontaneous phase transitions presented in Ref. 11. The model of Ref. 11 was developed to describe the second-order phase transition. It turns out that, if the one of two model parameters is suitably changed, then it is also able to describe the first-order transition. Therefore, in this way, we are able to compare the behavior of various measurable and nonmeasurable physical quantities in the first- and second-order phase transitions within one model. The attention will be directed to the specific behavior of the e_g electron distribution function, the order parameter, molecular field, free energy, heat capacity, and entropy. Then, we compare the predictions followed from this model calculations with the available experimental data.

The rest of the paper is organized as follows. In Sec. II we elucidate the nature of the molecular field, the e_g electron distribution function, and the order parameter in the first-order and second-order phase transitions. We indicate how this type of phase transition is expressed in terms of two parameters entering a used model. Then, we explain the extent to which the model parameters are associated with the first-order or second-order transitions. Section III presents investigations of the free energy. The entropy and the specific heat at the phase transition are calculated and the nature of the thermal hysteresis is explained. In Sec. IV the results of calculations are discussed in context of the various measurements. Finally, the controversy related to the order of transition is considered.

II. THE MOLECULAR FIELD

The condition for ferromagnetism is that the Mn moments become globally ordered. Weiss postulated a molecular field which causes this ordering. We will describe short-range interactions which are constituent elements of the molecular field. The two-level phenomenological model of both abrupt and continuous phase transitions was described previously.¹¹ A starting point in this model is a single $\text{Mn}^{3+}\text{-Mn}^{4+}$ pair of neighboring ions entering the $\text{Mn}^{3+}\text{-O}^{2-}\text{-Mn}^{4+}$ chain. At $T=0$ K, the e_g electron occupies the bonding state $|b\rangle$. In this state the e_g electron is equally distributed between two $d_{3z^2-r^2}$ orbitals on both Mn ions. With the increase of temperature the ground state admixes the nonbonding (excited)

states $|c\rangle$. This is the $d_{x^2-y^2}$ state located on any of two Mn ions. The one-electron free energies f for the ground and excited states can be expressed as

$$\begin{aligned} f_{|b\rangle} &= \varepsilon n^2 - \mu H - tR/2, \\ f_{|c\rangle} &= tR/2 - 2\varepsilon n + \varepsilon n^2 - k_B T \ln g + \mu H. \end{aligned} \quad (1)$$

where $n \in [0,1]$ is the electron distribution function, tR is the product of the hopping integral t between Mn ions multiplied by the Huang-Rhys factor R , ε is the Jahn-Teller energy, μ is the magnetic moment, $g=2$ accounts for the configurational degeneracy of state $|c\rangle$, and k_B is the Boltzmann constant. The origin of energy scale is taken in the middle between $|b\rangle$ and $|c\rangle$ levels (in Ref. 11 it was taken at level $|b\rangle$). With such a choice of the energy scale, the molecular field and the external magnetic field enter the free energy (6) in a symmetrical way. The Zeeman energy in the excited state is taken with the opposite sign with respect to the ground state because the electron in this state is bound only to one Mn ion (nonbonding state). When the electron occupies one of the $|c\rangle$ states, there is no correlation between the background electron (t_2) spins on neighboring Mn ions. This situation corresponds to the paramagnetic phase.

Using Eq. (1) one obtains the free energy F (the chemical potential) calculated per Mn^{3+} - Mn^{4+} pair:¹¹

$$F = \varepsilon n^2 - \mu H - k_B T \ln \left[1 + g \exp \left(- \frac{tR - 2\varepsilon n + 2\mu H}{k_B T} \right) \right]. \quad (2)$$

In the thermal equilibrium, the electron distribution n is determined by a minimization of the free energy F with respect to n , which gives

$$n = \frac{1}{\frac{1}{g} \exp \left(\frac{tR - 2\varepsilon n + 2\mu H}{k_B T} \right) + 1}. \quad (3)$$

Thus, Eq. (3) represents a self-consistent equation for n in which the partition function is related to a gap which is itself linearly related to n . Equation (3) resembles the form of the Fermi distribution function. The molecular field can be defined using the energy difference between the one-electron free energies:

$$\begin{aligned} f_{|c\rangle} - f_{|b\rangle} &= tR - 2\varepsilon n - k_B T \ln g + 2\mu H \\ &= 2\mu H_{mol}(T) + 2\mu H, \end{aligned} \quad (4)$$

where

$$H_{mol}(T) = \frac{tR - 2\varepsilon n - k_B T \ln g}{2\mu} \quad (5)$$

is the molecular field. It is seen $2\mu H_{mol}(0) = tR$ because $n = 0$ at $T = 0$ K. With this definition of $H_{mol}(T)$ the chemical potential is equal to

$$\begin{aligned} F &= \varepsilon n^2 - \mu H_{mol} - \mu H - k_B T \ln \\ &\times \left[1 + g \exp \left(- \frac{(2\mu H_{mol} + 2\mu H)}{k_B T} \right) \right]. \end{aligned} \quad (6)$$

Similar to known thermodynamical relation $(\partial F / \partial H)_T = -M$ one has

$$\left(\frac{\partial F}{\partial H_{mol}} \right)_T = -\mu(1 - 2n) = -M, \quad (7)$$

where M is the magnetization. $\Delta n = (1 - n) - n = 1 - 2n$ is the excess of the ferromagnetic phase over the paramagnetic one. Δn is the order parameter that distinguishes one phase from another. In case of the second-order transition $\Delta n > 0$ below the critical temperature T_C and $\Delta n = 0$ above T_C . Δn changes continuously with temperature between 1 and 0. Now, we shall consider the peculiarities of the first-order phase transition.

tR and ε are two unknown model parameters. These parameters influence all physical quantities. Practically, in case of the second-order phase transition, they are derived from the experimental value of T_C . It was shown¹¹ that $\varepsilon = 2k_B T_C$ and $tR = k_B T_C (2 + \ln g) - 2\mu H$. The relation $\varepsilon = 2k_B T_C$ follows from the requirement $dn/dT \rightarrow \infty$ when $T \rightarrow T_C$. This implies that the specific heat infinitely increases at the transition point. According to the Ehrenfest classification scheme, this is the λ transition. Hwang *et al.*¹² suggest that an abrupt change of the matrix element describing the electron hopping between Mn sites (in this paper, it corresponds to tR) may be responsible for the first-order phase transition. On the other hand, Novák *et al.*¹⁰ showed that variation of the exchange energy with the interatomic distances (it corresponds to ε , in this paper) may lead to discontinuity in magnetization. Indeed, the parameters tR and ε represent a different interaction but they are bound by the expression for the critical temperature. The critical temperature is itself material dependent. Below, we show that if we select $\varepsilon > 2k_B T_C$ then discontinuity in the magnetization and other physical quantities will appear. This leads to the change of the second-order phase transition to the first-order one. For the description of the second-order phase transition in $\text{La}_{1-x}\text{Ca}_x\text{MnO}_3$ crystal, we use the values of $\varepsilon = 289 \text{ cm}^{-1}$ and $tR = 392 \text{ cm}^{-1}$ from Ref. 11. They were adjusted to reproduce the critical temperature ≈ 210 K for the $\text{La}_{0.8}\text{Ca}_{0.2}\text{MnO}_3$ crystal.¹¹ In order to smoothly switch to the first-order character of the transition we keep the same value of tR and for the ε we take 293 cm^{-1} . Figure 1 shows the electron filling n [Eq. (3)] of the excited state $|c\rangle$. For the first-order transition this function is “folded” between the points L_p and H_f . L_p is abbreviation for the “low” temperature in the “paramagnetic” phase and H_f is abbreviation for the “high” temperature in the “ferromagnetic” phase. The values of n between these points are not accessible for the system. In this range dn/dT possesses unphysical negative value. This is due to a failure of thermodynamic stability in the system. The second derivative $\partial^2 F / \partial n^2$ is negative and the free energy in this range of n is not at minimum. In the second-order phase transition, the filling n is a continuous

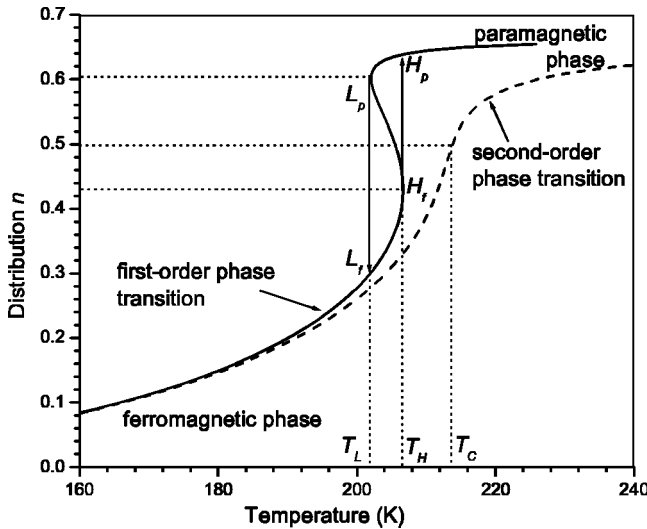


FIG. 1. The electron filling n of the excited state $|c\rangle$. For the first-order transition this function is “folded” between the points L_p and H_f . The values of n between these points are not accessible for the system. The model parameters are $\varepsilon = 293 \text{ cm}^{-1}$, $tR = 392 \text{ cm}^{-1}$ for the first-order transition and $\varepsilon = 289 \text{ cm}^{-1}$, $tR = 392 \text{ cm}^{-1}$ for the second-order phase transition.

function of temperature and $n = 1/2$ corresponds to T_C . In the first-order phase transition usually there are high-temperature critical point T_H and low-temperature critical point T_L . Hwang *et al.*¹² note [observing $(\text{LaPr})_{0.7}\text{Ca}_{0.3}\text{MnO}_3$ and $(\text{LaY})_{0.7}\text{Ca}_{0.3}\text{MnO}_3$] that for manganites with relatively high critical temperature the transition is likely to be of the second order, while in those with lower critical temperature is of the first order. Indeed, Fig. 1 shows the lowering of the critical temperature for the first order transition as compared with the second-order one, i.e., $T_L, T_H < T_C$. We note that we intentionally adjust such value of ε which gives hysteresis of about $T_H - T_L \approx 5 \text{ K}$. Near T_C , the e_g electrons strongly absorb the thermal energy and the configuration change $|b\rangle \rightarrow |c\rangle$. The derivative dn/dT exhibits the resonance peak at this temperature. Figure 2 shows the order parameter Δn . It is seen that at T_H and T_L it possesses different finite values. It exhibits the hysteresis in cooling and warming cycles. In Fig. 3 we draw the molecular field H_{mol} multiplied by 2μ . It exhibits the discontinuity at T_H . The molecular field varies with temperature in a similar way as an energy gap in the BSC theory of superconductors. The molecular field originates from the covalency and the electron-phonon interaction taken in the first order of perturbation theory whereas the BSC gap originates from the electron-phonon interaction taken in the second order of perturbation theory.

III. THE HYSTERESIS

Hysteresis is often caused by phase transitions that involve abrupt changes in certain parameters of a thermodynamic system. The thermodynamic behavior of the system can be described in terms of its free energy. In particular, the Helmholtz free energy describes the energy liberated or ab-

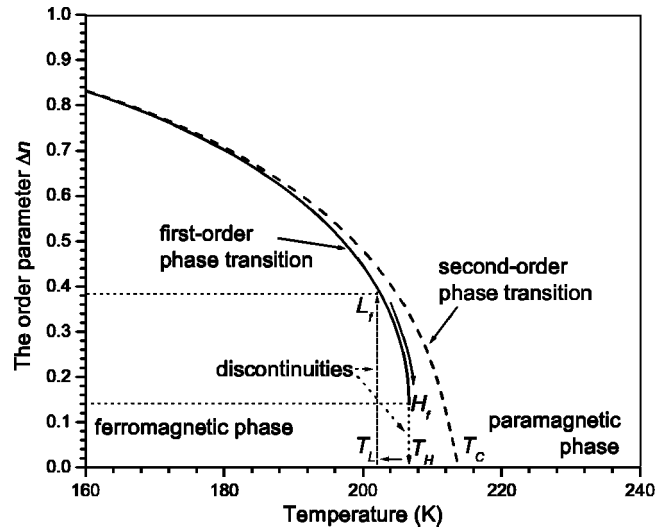


FIG. 2. The order parameter $\Delta n = 1 - 2n$ vs temperature. The hysteresis is denoted by the arrows in the cooling-warming cycles.

sorbed during a phase transition at constant volume and temperature. Using expression (2) the mechanics of the phase transitions, and therefore hysteresis, will be considered. Figure 4 shows the free energy [Eq. (2)] vs temperature. Drawing this figure we expressed n as a function of T using Eq. (3). The discontinuity of the free energy at T_L and T_H can be observed. The finite difference ΔF between the old and new minima is the latent heat of the phase transition.

The energy F is discontinuous function of filling n . This is shown in Fig. 5. The values of n did not minimize F , i.e., $\partial^2 F / \partial n^2 < 0$ between the points H_f and L_p . The last two graphs explain the nature of hysteresis. Suppose we follow warming cycle between the points L_f and H_f . According to Fig. 4 two curves of the free energy cross each other around $T \approx 205.5 \text{ K}$ (this corresponds to filling $n = 1/2$). A question arises, why the system passing this crossing point does not follow the lower free energy curve with the temperature increase? To find the correct explanation one should note that

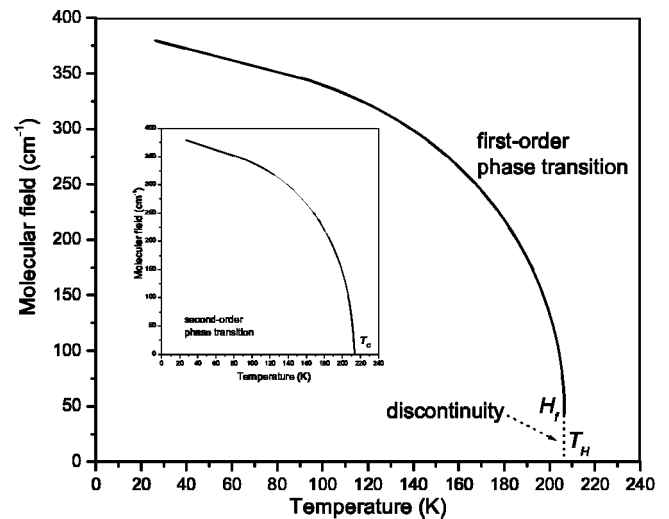


FIG. 3. The molecular field H_{mol} multiplied by 2μ vs temperature.

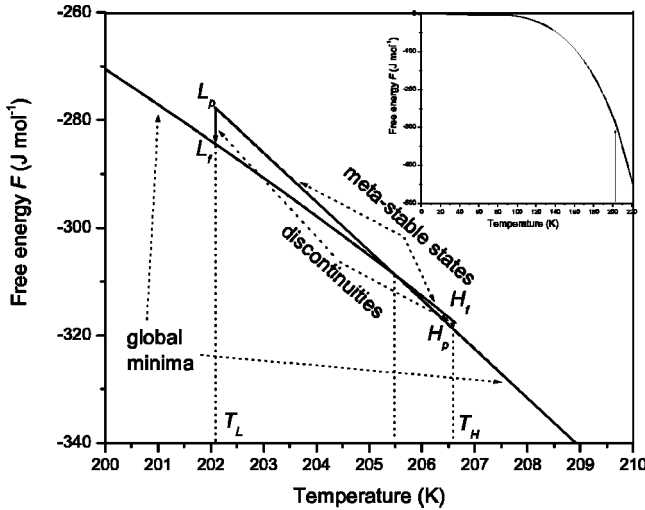


FIG. 4. The free energy F [Eq. (2)] vs temperature. The inset shows F in the wide temperature range and the place of the feature shown in the main graph is indicated by arrow. Apart from this feature the function $F(T)$ is similar in the first- and second-order phase transitions.

in such a case there is discontinuous entropy change (the slope of F at $T \approx 205.5$ K in Fig. 4). Thus, at the crossing point, an abrupt change of the electronic configuration n , i. e., some structural change without any energy gain is required. As it is seen in Fig. 5, the free energy continuously decreases between the points L_f and H_f with the increase of n , or equivalently, with temperature increase. Therefore, the system prefers to continuously decrease its free energy with the temperature increase, instead of undergoing the configuration change without the energy gain at the crossing point. However, when the system reaches the point H_f there is no way to decrease its energy without the discontinuous electronic configuration change. This causes the discontinuity of the order parameter Δn . The similar consideration is also applied to the cooling cycle between the points H_p and L_p .

Using the expression for the free energy F one finds the entropy S

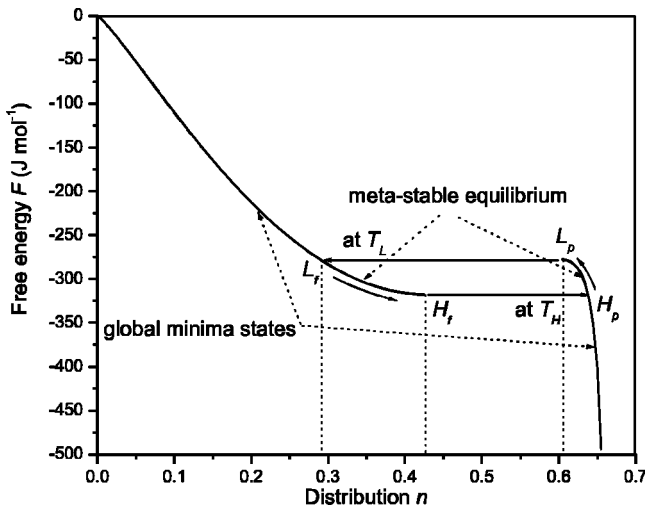


FIG. 5. The free energy F vs distribution n .

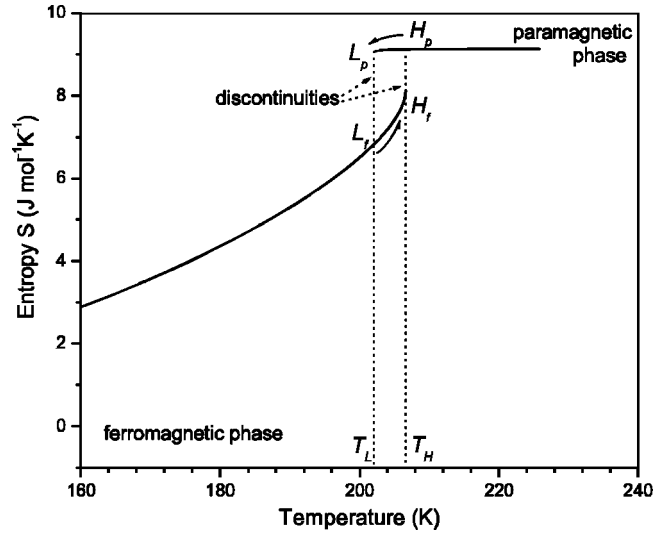


FIG. 6. The entropy S vs temperature.

$$S = - \left(\frac{\partial F}{\partial T} \right)_V = -k_B [-n \ln g + n \ln n + (1-n) \ln(1-n)]. \quad (8)$$

In Fig. 6 the thermal hysteresis in the entropy values between the critical temperatures T_L and T_H is clearly seen. Taking into account the explicit expression for the entropy S one can calculate the electronic contribution to the heat capacity C_V :

$$C_V(T) = T \left(\frac{\partial S}{\partial T} \right)_V = (tR - 2\varepsilon n + 2\mu H) \frac{dn}{dT}, \quad (9)$$

where

$$\frac{dn}{dT} = \frac{n(1-n)[tR - 2\varepsilon n + 2\mu H]}{T[k_B T - 2\varepsilon n(1-n)]}. \quad (10)$$

Figure 7 shows the calculated specific heat. The peak of the specific heat was intentionally cut. Because dn/dT behaves

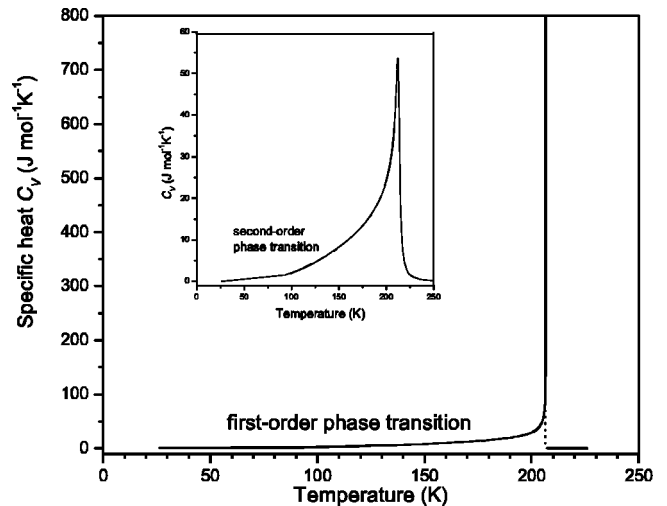


FIG. 7. The electronic specific heat C_V vs temperature. The height of the specific heat was intentionally cut. Inset shows the specific heat for the second-order transition.

as a δ function at T_H the specific heat is around an order of magnitude larger than it is shown in this figure. Normally, the specific heat calculated for the second-order transition is broader and smaller because dn/dT is finite. However, if at the point T_C , the derivative $dn/dT \rightarrow \infty$ the specific heat in the second-order transition is reminiscent of the one in the first-order transition. In the vicinity of T_C , the heat $C_V \Delta T$ drives electrons strongly from the state $|b\rangle$ to $|c\rangle$ or, equivalently, increases the entropy by ΔS instead of raising the crystal temperature.

IV. RESULTS AND DISCUSSION

The hysteresis loops are often seen in experiments at first-order phase transformations when the system goes out of equilibrium. We show that such range of values of the occupancy n for which the crystals exhibit hysteresis exist. Within the temperature where the metastable states exist, the order parameter Δn , the free energy F , and entropy S depend on the system history, i.e., whether T was increasing or decreasing when it attained the metastable range between T_L and T_H . Recall that the order parameter distinguishes one phase from another; therefore the distinct values of Δn that admit distinct equilibrium states also distinguish the different phases of the system. In the first order when T decreases the phenomenon known as supercooling can occur. This is because the original minimum represents a metastable equilibrium. As T decreases further, or the crystal is perturbed by either internal or external fluctuations, the system finally evolves at T_L into the global minimum that represents the true energetically stable state. This liberates the latent heat that was stored in the metastable state. Similarly, when the crystal in the ordered state is heated up again to a temperature of around T_H it absorbs this latent heat, a phenomenon called reheating.

In the perovskites, such as $\text{La}_{1-x}\text{Ca}_x\text{MnO}_3$, the ferromagnetic and paramagnetic phases may exist simultaneously. The ferromagnetic state to paramagnetic state ratio depends on temperature and pressure.^{13–20} The hopping parameter tR depends on the distance between neighboring Mn ions and the Jahn-Teller energy ε depends on the Mn-O distance. Therefore by the application of external pressure it is possible to tune T_L and T_H . When the hysteresis loop is reduced to single line, i.e., when $T_L = T_H = T_C$ there is a border between the first- and second-order phase transitions. At this temperature $dn/dT \rightarrow \infty$. In the first-order process $dn/dT \rightarrow \infty$ at the critical temperatures (discontinuity in filling n) whereas dn/dT is positive and finite in the second-order process at T_C . The ground $|b\rangle$ and excited $|c\rangle$ states possess the equilibrium at the different displacement coordinates. This is the reason why the Jahn-Teller distortion plays an essential role in the phase transition in the perovskite-type ferromagnetics. The adiabatic approximation breaks around the transition temperature because the electronic configuration is strongly coupled to the vibrations of atoms. As a consequence, the dn/dT exhibits a resonance.

Zhao *et al.*⁷ using the experimental data regarding the specific heat, expansion coefficient, and dT_C/dP concluded that these data satisfy the Ehrenfest equation.²¹ Thus, they

concluded that the FP transition is the second-order one. We want only to mention that from the form of Eq. (9) it follows that the experimental peak positions of the specific heat are slightly below ($\approx 1-1.5$ K) the T_C point. On other hand, Gordon *et al.*⁶ who analyzed similar data concluded that the experimental data satisfy rather the Clausius-Clapeyron equation.²¹ Therefore, they concluded that the FP transition is the first-order one. Ghivelder *et al.*⁵ from the height of measured specific heat suggest the first-order process. Indeed, the calculated specific heat for the first- and second-order transitions (see Fig. 7) differs remarkably. The specific-heat peak for the first-order is much higher than that observed by Ghivelder *et al.* Additionally, the magnetization measured there seems to be a continuous function of temperature. Therefore, we believe that they observed the second-order phase transition.

The measurements of magnetization^{6,9} are used to investigate the order of phase transition. Using the results of the general theory for the second-order phase transition given by Landau, the Arrott graph (H/M vs M^2) is plotted. If the slope of this graph is positive the transition is of the second order. In this connection we mention that Landau theory is based on the series expansion of the free energy over the order parameter $\Delta n = M/\mu$ which is valid for a range of temperature just below T_C . However, as it is seen in Fig. 2 the order parameter is discontinuous at T_H (where phase transformation occurs). Therefore, the expansion, similar to that in the Landau theory, is questionable. Hence, the application of the Arrott graph for the investigation of the first-order transition needs to be justified. Additionally, in the Landau theory, phase transitions correspond to the systems passing through states of thermodynamic equilibrium, when states are nondegenerate on both sides of the transition point. In the present case, there are the configurational degeneracy in the paramagnetic states. The ground and excited states have minima at different displacement coordinates. This creates the additional feature which distinguishes the Landau consideration from the present model. The explanation of the magnetization measurements in $\text{La}_{0.67}\text{Ca}_{0.33}\text{MnO}_3$ by Lynn *et al.*⁴ is very controversial. The magnetization loop on warming and cooling observed there [in Fig. 2(b)] exhibits a temperature irreversibility of 5 K. But on the other hand this magnetic loop is very different in shape from that for Δn shown here in Fig. 2. It extends down well below the critical temperature (to around 100 K). Similar hysteresis loop was observed for the electrical resistivity in Ref. 22 [Fig. 1(a) there]. In both works, it was interpreted as sign of the first-order phase transition. However, the specific heat measured in Ref. 22 (Fig. 2 there) is quite broad and low, pointing to the second-order character of the transition. Therefore, this problem requires further investigation. We only mention that from the computational point of view the warming and cooling processes do not change the interaction parameters such as tR and ε . Therefore, the hysteresis loop should be similar to that in Fig. 2. However, if some magnetic domains are formed in the material then, due to presence of some kinds of “magnetic resistivity,” one can expect the loop observed in Refs. 4 and 22.

In conclusion, we described the model (involving two

parameters) of the FP phase transition of the first and second order. The transition is always accompanied by the electron configuration change. The configuration change is at the energy $k_B T_{critical} = (tR - 2\varepsilon\Delta n + 2\mu H/\ln g)$, where Δn should be taken for the appropriate type of transition. The partition function n , depending on the model parameters tR and ε , can describe, as a function of T , the gradual or discontinuous transition between the ferromagnetic and paramagnetic phases. In particular, we explain why the critical temperature is expected to be lower in the first-order transition as compared with the second-order transition. In order to determine the character of the phase transition, it is necessary to consider simultaneously the behavior of the different physical

quantities near the transition point. However, when the thermal hysteresis is negligible, say 1 K, the observed specific heat, magnetization, and the expansion coefficient will be influenced (broadened) due to inhomogeneity of $A_{1-x}M_x\text{MnO}_3$ crystals. In this case, the specific heat and magnetization associated with the first-order transition can be similar to those in the second-order transition.

ACKNOWLEDGMENT

We express our most sincere thanks to Professor A. Suchocki for his many useful suggestions and the constructive criticism.

*Electronic address: biern@ifpan.edu.pl

¹Localized to Itinerant Electronic Transition in Perovskite Oxides, in *Structure and Bonding*, edited by J.B. Goodenough (Springer-Verlag, Berlin, 2001), Vol. 98.

²N. Tsuda, K. Nasu, A. Fujimori, and K. Siratori, *Electronic Conduction in Oxides*, 2nd ed. (Springer-Verlag, Berlin, 2001).

³E. Dagotto, T. Hotta, and A. Moreo, *Phys. Rep.* **344**, 1 (2001).

⁴J.W. Lynn, R.W. Erwin, J.A. Borchers, Q. Huang, A. Santoro, J.L. Peng, and Z.Y. Li, *Phys. Rev. Lett.* **76**, 4046 (1996).

⁵L. Ghivelder, I. Abrego Castillo, N.McN. Alford, G.J. Tomka, P.C. Riedi, J. MacManus-Driscoll, A.K.M. Akther Hossain, and L.F. Cohen, *J. Magn. Magn. Mater.* **189**, 274 (1998).

⁶J.E. Gordon, C. Marcenat, J.P. Franck, I. Isaac, G. Zhang, R. Lortz, C. Meingast, F. Bouquet, R.A. Fisher, and N.E. Phillips, *Phys. Rev. B* **65**, 024441 (2001).

⁷G. Zhao, M.B. Hunt, and H. Keller, *Phys. Rev. Lett.* **78**, 955 (1997).

⁸R.H. Heffner, L.P. Le, M.F. Hundley, J.J. Neumeier, G.M. Luke, K. Kojima, B. Nachumi, Y.J. Uemura, D.E. MacLaughlin, and S.W. Cheong, *Phys. Rev. Lett.* **77**, 1869 (1996).

⁹J. Mira, J. Rivas, F. Rivadulla, C. Vázquez-Vázquez, and M.A. López-Quintela, *Phys. Rev. B* **60**, 2998 (1999).

¹⁰P. Novák, M. Maryško, M.M. Savosta, and A.N. Ulyanov, *Phys. Rev. B* **60**, 6655 (1999).

¹¹S.W. Biernacki, *Phys. Rev. B* **66**, 094405 (2002).

¹²H.Y. Hwang, S.W. Cheong, P.G. Radaelli, M. Marezio, and B. Batlogg, *Phys. Rev. Lett.* **75**, 914 (1995).

¹³P. Dai, J. Zhang, H.A. Mook, S.-H. Liou, P.A. Dowben, and E.W. Plummer, *Phys. Rev. B* **54**, R3694 (1996).

¹⁴P.G. Radaelli, D.E. Cox, M. Marezio, S.-W. Cheong, P.E. Schiffer, and A.P. Ramirez, *Phys. Rev. Lett.* **75**, 4488 (1995).

¹⁵P.G. Radaelli, G. Iannone, M. Marezio, H.Y. Hwang, S.W. Cheong, J.D. Jorgensen, and D.N. Argyriou, *Phys. Rev. B* **56**, 8265 (1997).

¹⁶J.J. Neumeier, T.T.M. Palstra, S.W. Cheong, and B. Batlogg, *Phys. Rev. B* **52**, R7006 (1995).

¹⁷H.Y. Hwang, T.T.M. Palstra, S.W. Cheong, and B. Batlogg, *Phys. Rev. B* **52**, 15 046 (1995).

¹⁸J.M. De Teresa, M.R. Ibarra, J. Blasco, J. Garcia, C. Marquina, P.A. Algarabel, Z. Arnold, K. Kamenev, C. Ritter, and R. von Helmolt, *Phys. Rev. B* **54**, 1187 (1996).

¹⁹V. Laukhin, J. Fontcuberta, J.L. Garcia-Muñoz, and X. Obradors, *Phys. Rev. B* **56**, R10 009 (1997).

²⁰Y.S. Wang, A.K. Heilman, B. Lorenz, Y.Y. Xue, C.W. Chu, J.P. Franck, and W.M. Chen, *Phys. Rev. B* **60**, R14 998 (1999).

²¹L.D. Landau and E.M. Lifshitz, *Statistical Physics* (Nauka, Moscow, 1964), Chaps. 8 and 14.

²²M.T. Fernández-Dáz, J.L. Martínez, J.M. Alonso, and E. Herrero, *Phys. Rev. B* **59**, 1277 (1999).